

The vector coupling $\alpha_V(r)$ and the scales r_0, r_1 from the bottomonium spectrum

A.M. Badalian*

State Research Center, Institute of Theoretical and Experimental Physics, Moscow 117218, Russia

B.L.G. Bakker†

*Department of Physics and Astronomy,
Vrije Universiteit, Amsterdam, The Netherlands*

(Dated: March 13, 2013)

With the use of the relativistic string Hamiltonian we study the universal static potential $V_{\text{st}}(r)$ and the force, which are fully determined by two fundamental parameters: the string tension $\sigma = 0.18 \pm 0.02 \text{ GeV}^2$ and the QCD constants $\Lambda_{\overline{\text{MS}}}(n_f)$, taken from pQCD, while the infrared (IR) regulator M_B is expressed via the string tension. The vector couplings $\alpha_V(r)$ in the static potential and $\alpha_F(r)$ in the static force, as well as the characteristic scales, $r_1(n_f = 3)$ and $r_0(n_f = 3)$, are calculated and compared to lattice data. The result $r_0 \Lambda_{\overline{\text{MS}}}(n_f = 3) = 0.77 \pm 0.03$ is obtained for $M_B = (1.15 \pm 0.02) \text{ GeV}$, while in bottomonium better agreement with experiment is reached for $\Lambda_{\overline{\text{MS}}}(n_f = 3) = (325 \pm 15) \text{ MeV}$ and the frozen value $\alpha_V = 0.57 \pm 0.02$. The mass splittings $\bar{M}(1D) - \bar{M}(1P)$ and $\bar{M}(2P) - \bar{M}(1P)$ are shown to be sensitive to the IR regulator used. The masses $M(1^3D_3) = 10170(2) \text{ MeV}$ and $M(1^3D_1) = 10154(3) \text{ MeV}$ are predicted.

I. INTRODUCTION

The Hamiltonian formalism may be considered as a powerful tool to study such hadron properties as meson spectroscopy, including high excitations, hyperfine and fine structure splittings of different meson multiplets, leptonic widths, and radiative and strong meson de-

*Electronic address: badalian@itep.ru

†Electronic address: b.l.g.bakker@vu.nl

cays. For decades, different phenomenological Hamiltonians were used in constituent quark models, and some of them were rather successful in predictions of meson properties for low-lying states [1]-[5]. However, in such models the quark-antiquark potentials contain a large number of arbitrary parameters like constituent quark masses, variable values of the string tension and the QCD constant Λ , as well as a overall additive fitting constant. Meanwhile, the relativistic string Hamiltonian (RSH) H_R , which was derived from the gauge-invariant meson Green's function with the use of the QCD Lagrangian [6], contains only fundamental parameters: the quark current masses, the string tension σ fixed by the slope of the Regge trajectories for light mesons, and the QCD constants $\Lambda(n_f)$, taken from perturbative QCD (pQCD). It is important that in RSH the spin-independent static $q\bar{q}$ potential $V_{\text{st}}(r)$ is applicable for the quarks with arbitrary masses (including $m_q = 0$). It is defined via the vacuum average over the Wilson loop $\langle W(C) \rangle$ and has to be a universal. In Refs. [6]-[9] the only approximation made is that $\langle W(C) \rangle$ is taken in the form of the minimal area law, which appears to be a good approximation for the separations $r \gtrsim T_g \sim 0.15$ fm, where T_g is the vacuum correlation length. Later the behavior of the strong coupling in the IR region was studied in Ref. [10], where it was shown that the IR regulator is not a new parameter but expressed via the string tension.

It was shown that the nonperturbative (NP) part of the static potential has a linear behavior beginning at $r \gtrsim 0.2$ fm, while at short distances, $r \lesssim 0.15$ fm, the NP potential is proportional to r^2 [11]. Such a deviation from linear behavior, in a very narrow region, gives a small effect for all mesons, with the exception of $\Upsilon(1S)$, which has a small size, $R \sim 0.20$ fm, and for $\Upsilon(1S)$ some corrections to the confining potential should be taken into account.

This universal quark-antiquark potential is additive, containing the linear confining part and the gluon-exchange (GE) part:

$$V_{\text{st}}(r) = \sigma r + V_{\text{GE}}(r), \quad (1)$$

which is confirmed by the Casimir scaling, studied analytically [12] and numerically on the lattice [13]. Here the string tension is fixed by the slope of the Regge trajectories of the light mesons, being known to good accuracy, $\sigma = 0.180 \pm 0.002$ GeV².

In the gluon-exchange (GE) potential (1)

$$V_{\text{GE}}(r) = -\frac{4}{3} \frac{\alpha_V(r)}{r}, \quad (2)$$

the vector coupling in coordinate space $\alpha_V(r)$, is defined through the vector coupling $\alpha_V(q^2)$ in the momentum space,

$$\alpha_V(r) = \frac{2}{\pi} \int_0^\infty dq \frac{\sin(qr)}{q} \alpha_V(q). \quad (3)$$

For large q^2 there exists an important relation between $\alpha_V(q^2)$ in the momentum space and the conventional $\alpha_s(q^2)$ in the $\overline{\text{MS}}$ renormalization scheme [14]. In pQCD the cross sections and other observables are predicted in terms of this coupling.

The coupling $\alpha_s(q^2)$ is measured at different (large) energy scales q^2 and the values obtained are usually presented at a common energy scale, equal to the Z -boson mass, $M_Z = 91.188$ GeV. From numerous experimental studies, like the hadronic widths of the Z^0 boson, the τ -lepton decays, radiative $\Upsilon(1S)$ decays, jet production in the e^+e^- annihilation, and the structure functions in deep inelastic scattering, the world average value of the strong coupling is now determined with a good accuracy, $\alpha_s(m_Z) = 0.1184 \pm 0.0007$ [15, 16]. As a consequence, the QCD constant $\Lambda_{\overline{\text{MS}}}(n_f = 5)$ is also known with a good accuracy. Then, using the matching procedure at the quark mass thresholds, the other $\Lambda_{\overline{\text{MS}}}(n_f)$ for $n_f = 3, 4$ are calculated and the three-loop calculations give the following $\Lambda_{\overline{\text{MS}}}(n_f)$ [16]:

$$\begin{aligned} \Lambda_{\overline{\text{MS}}}(n_f = 3) &= (339 \pm 10) \text{ MeV}, \\ \Lambda_{\overline{\text{MS}}}(n_f = 4) &= (296 \pm 10) \text{ MeV}, \\ \Lambda_{\overline{\text{MS}}}(n_f = 5) &= (213 \pm 8) \text{ MeV}. \end{aligned} \quad (4)$$

This result is also important for the vector coupling since the “vector” constants $\Lambda_V(n_f)$ are defined via $\Lambda_{\overline{\text{MS}}}(n_f)$ [14]. They appear to be significantly larger, e.g. $\Lambda_V(n_f = 3) = (500 \pm 15) \text{ MeV}$ corresponds to the value $\Lambda_{\overline{\text{MS}}}(n_f = 3) = (339 \pm 10) \text{ MeV}$ from Eq. (4) (see Sect. III).

The analysis of the $V_{\text{GE}}(r)$ shows that perturbative effects determine $\alpha_V(r)$ only at very small distances $r \lesssim 0.06$ fm [17] and this result was confirmed by the lattice measurements of the static potential [18]. It means that in the GE potential NP effects become important, beginning from very short distances, and one needs to determine the vector coupling in the infrared (IR) region.

For heavy quarkonia the importance of NP effects was understood already in 1975, just after the discovery of the charmed quark, when the Cornell group introduced the linear + Coulomb potential with rather large vector coupling, $\alpha_V = \text{constant} = 0.39$ [1], in which

the asymptotic freedom (AF) behavior was neglected. However, future studies have shown that the AF behavior of the vector coupling is very important, in particular for the wave functions (w.f.) and its derivatives at the origin [19], [20]. When the AF behavior is taken into account, even larger asymptotic values of α_V were used in phenomenological models, e.g. the value ~ 0.60 in Refs. [3], [20] and such a large spread in these values occurs because of a different choice of the fitting parameters.

On the fundamental level not many theoretical attempts were undertaken to determine the strong coupling in the IR region. On the phenomenological level a regularization of the strong coupling was suggested long ago, with the prescription to introduce the IR regulator into the logarithm $\ln \frac{q^2}{\Lambda^2}$, changing it into $\ln \left(\frac{q^2 + M_{2g}^2}{\Lambda^2} \right)$ [21]. This IR regulator was interpreted as an effective two-gluon mass $M_{2g} = 2m_g$. However, in QCD the appearance of the gluon mass is forbidden by gauge invariance and the meaning and the value of the IR regulator remained unsolved for many years.

Recently a new result was obtained within background perturbation theory (BPTh) [10], where indeed the type of the logarithm, as in Ref. [21], was derived with the IR regulator (denoted as M_B), expressed through the string tension, so that M_B is not an additional parameter. This NP regulator has the meaning of the mass of the two-gluon system, connected by the fundamental string (white object) and its value is determined by the equation: $M_B^2 = 2\pi\sigma$. It gives $M_B \simeq (1.06 \pm 0.11)$ GeV for $\sigma \sim 0.180$ GeV², the accuracy of the calculations being determined by the accuracy of the WKB method used ($\sim 10\%$). In [22] the IR regulators were studied in so-called “massive” perturbative QCD, developed within Analytic Perturbation Theory. Their values obtained in two-loop calculations, also lie in the range $(0.9 - 1.2)$ GeV.

However, for a given $\Lambda_{\overline{\text{MS}}}(n_f = 3)$ the variation of the regulator M_B in the range $1.0 - 1.15$ GeV gives rise to large differences in the asymptotic (frozen) value of the vector coupling, called α_{crit} in Ref. [3]: $\alpha_V(q = 0) = \alpha_V(r \rightarrow \infty) = \alpha_{\text{crit}}(n_f = 3)$. For example, taking the perturbative central value, $\Lambda_{\overline{\text{MS}}}(n_f = 3) = 339$ MeV from Eq. (4) and the corresponding $\Lambda_V(n_f = 3) = 1.4753 \Lambda_{\overline{\text{MS}}}(n_f = 3) = 500$ MeV, one obtains $\alpha_{\text{crit}}(2\text{-loop})$ equal to the large value 0.82 for $M_B = 0.95$ GeV and a smaller value 0.635 for the larger $M_B = 1.15$ GeV. Meanwhile, the critical value of the vector coupling is of special importance for the meson spectrum and therefore one needs to determine the IR regulator, as well as $\Lambda_{\overline{\text{MS}}}(n_f = 3)$, with great accuracy.

Notice that smaller values of $\Lambda_V(n_f = 3)$ were used in Refs. [3, 23] and in pQCD $\Lambda_{\overline{\text{MS}}}(n_f = 3) = (292 \pm 29)$ MeV, smaller than given in Eq. (4), was calculated in Ref. [24]. On the lattice the small value $\Lambda_{\overline{\text{MS}}}(n_f = 0) = (245 \pm 20)$ MeV was obtained in quenched QCD [25].

Our goal here is to study how the properties of the vector coupling and the bottomonium spectrum depend on the IR regulator and $\Lambda_V(n_f = 3)$ used. We will show that the meson spectrum is governed by the ratio $\eta^2 = \frac{M_B^2}{\Lambda_V^2}$ (or $\tilde{\eta}^2 = \frac{M_B^2}{\Lambda_{\overline{\text{MS}}}^2}$). Then for large $\Lambda_V(n_f = 3) \sim 500$ MeV, as in pQCD, the value of the IR regulator $M_B = (1.15 \pm 0.02)$ GeV appears to be preferable, in agreement with the prediction from [10].

II. RELATIVISTIC STRING HAMILTONIAN

The RSH H_R was derived from the gauge-invariant meson Green's function, performing several steps (see [6, 9]). For a meson $q_1\bar{q}_2$ with the masses m_1 and m_2 the RSH contains several terms,

$$H_R = H_0 + H_{\text{SD}} + H_{\text{str}} + H_{\text{SE}}, \quad (5)$$

where the part H_{SD} refers to the spin-dependent potential, like hyperfine or fine-structure interactions; the term H_{str} comes from the rotation of the string itself and determines the so-called string corrections for the states with $l \neq 0$, while H_{SE} comes from the NP self-energy contribution to the masses of the quark and the antiquark [26]. All these terms appear to be much smaller than the unperturbed part H_0 for all mesons, and therefore can be considered as a perturbation. The part H_0 is derived in the form,

$$H_0 = \frac{\omega_1}{2} + \frac{\omega_2}{2} + \frac{m_1^2}{2\omega_1} + \frac{m_2^2}{2\omega_2} + \frac{\mathbf{p}^2}{2\omega_{red}} + V_{\text{st}}(r). \quad (6)$$

Here the variables ω_i are the kinetic energy operators, which have to be determined from the extremum condition, $\frac{\partial H_0}{\partial \omega_i} = 0$, giving

$$\omega_i = \sqrt{m_i^2 + \mathbf{p}^2} \quad (i = 1, 2), \quad (7)$$

and therefore Eq. (6) can be rewritten as

$$H_0 = \sqrt{m_1^2 + \mathbf{p}^2} + \sqrt{m_2^2 + \mathbf{p}^2} + V_{\text{st}}(r). \quad (8)$$

This form of H_R is applied to heavy-light mesons, while for bottomonium it is very simplified. Among all mesons the bottomonium spectrum is of a special importance, since it has the

largest number of levels below the open flavor threshold. Altogether there are nine $b\bar{b}$ multiplets with $l = 0, 1, 2, 3$ and seven of them were already observed, and one can use this extensive information to test the static quark-antiquark potential. An additional piece of information on the coupling $\alpha_s(\mu)$ at different scales μ may be obtained from studies of the hyperfine and fine structure effects in bottomonium [27].

By derivation, the quark (antiquark) mass m_i in the RSH is equal to the current quark (antiquark) mass, $\bar{m}_i(\bar{m}_i)$ in the $\overline{\text{MS}}$ renormalization scheme, and therefore it is not a fitting parameter. In the case of a heavy quark one needs to take into account corrections perturbative in α_s , i.e., to use the pole mass of a heavy quark, which is taken here to two-loop accuracy [1, 15]:

$$m_Q = \bar{m}_Q(\bar{m}_Q) \left\{ 1 + \frac{4}{3} \frac{\alpha_s(\bar{m}_Q)}{\pi} + \xi_2 \left(\frac{\alpha_s}{\pi} \right)^2 \right\}, \quad (9)$$

where ξ_2 may be taken from [15]. For the b quark the pole mass can symbolically be written as $m_b(\text{pole}) = \bar{m}_b(\bar{m}_b)(1 + 0.09 + 0.05)$, where the second and third terms come from the α_s and α_s^2 corrections. In our calculations $m_b(\text{pole}) = (4.81 \pm 0.03)$ GeV is used, which corresponds to the conventional current mass $\bar{m}_b(\bar{m}_b) = (4.22 \pm 0.03)$ GeV.

For bottomonium the calculated string and self-energy terms are very small, ≤ 1 MeV, and therefore $H_R = H_0 + H_{\text{SD}}$, where from Eq. (8) H_0 ,

$$H_0 = 2\sqrt{m_b^2 + \mathbf{p}^2} + V_{\text{st}}(r), \quad (10)$$

has a kinetic term, which formally coincides with that in the spinless Salpeter equation (SSE), often used in relativistic models with constituent quark masses. Such a coincidence between the kinetic terms in the SSE and the RSH, which was derived from first principles, possibly explains why the use of the SSE was successful in Refs. [2, 3, 5].

An important feature of the RSH is that it does not contain an overall additive (fitting) constant, which is usually present in models with constituent quark masses and also in the lattice static potential [24]. Notice that the presence of such a constant in the meson mass violates the linear behavior of the Regge trajectories for light mesons. On the contrary, with the use of H_R linear Regge trajectories can be easily derived with the correct slope and intercept [9] (later we use the string tension $\sigma = 0.180 \pm 0.002$ GeV², extracted from the slope of the Regge trajectories for light mesons). In heavy quarkonia low-lying states do not lie on linear Regge trajectories, because of strong GE contributions.

III. THE VECTOR COUPLING IN MOMENTUM SPACE

First we consider the vector coupling $\alpha_V(q)$ in momentum space, taking it in two-loop approximation, where the coupling does not depend on the renormalization scheme. For $\alpha_V(q^2)$ we shall use the notation $\alpha_B(q^2)$, bearing in mind that it contains the IR regulator M_B , determined as in BPTH [10]:

$$\alpha_B(q^2) = \frac{4\pi}{\beta_0 t_B} \left(1 - \frac{\beta_1}{\beta_0^2} \frac{\ln t_B}{t_B} \right), \quad (11)$$

where M_B , entering the logarithm $t_B = \ln \frac{(q^2 + M_B^2)}{\Lambda_V^2}$, is not a new parameter but determined via the string tension [10]:

$$M_B^2 = 2\pi\sigma. \quad (12)$$

Here σ is the string tension in the fundamental representation, $\sigma = (0.180 \pm 0.002) \text{ GeV}^2$. The accuracy of the relation (12) is determined by the accuracy of the WKB approximation used in Ref. [10], which is estimated to be $\leq 10\%$. Therefore

$$M_B = (1.06 \pm 0.11) \text{ GeV}. \quad (13)$$

The analysis of the bottomonium spectrum shows that the larger values, $M_B = (1.15 - 1.20) \text{ GeV}$, are preferable, if a large $\Lambda_V(n_f = 3) = (500 \pm 15) \text{ MeV}$, corresponding to the pQCD value $\Lambda_{\overline{\text{MS}}}(n_f = 3) = (339 \pm 10)$ from Eq. (4), is taken, while for the smaller $M_B = (1.05 \pm 0.05) \text{ GeV}$ and the same Λ_V one obtains a too large $2P - 1P$ splitting and also a large b-quark pole mass, $m_b = 4.90 \text{ GeV}$.

The vector coupling $\alpha_B(q^2)$ has the AF property at large momentum q^2 , where the “vector” constant $\Lambda_V(n_f)$ is expressed through the conventional $\Lambda_{\overline{\text{MS}}}(n_f)$. This connection between both Λ s follows from the relation between the strong couplings (valid at large q^2), established in Ref. [14],

$$\alpha_V(q^2) = \alpha_s(q^2) \left(1 + \frac{a_1}{4\pi} \alpha_s(q) \right) \approx \frac{\alpha_s(q)}{\left(1 - \frac{a_1}{4\pi} \alpha_s(q) \right)}. \quad (14)$$

Here $a_1 = \frac{31}{3} - \frac{10}{9}n_f$. For our purpose it is enough to use in Eq. (14) the one-loop approximation for both couplings: $\alpha_B = \frac{4\pi}{\beta_0} \ln \frac{q^2}{\Lambda_V^2}$ with $\beta_0 = 11 - \frac{2}{3}n_f$ and the analogous expression for $\alpha_s(q)$. From this equation it follows that $\ln \frac{q^2}{\Lambda_V^2} = \left(\ln \frac{q^2}{\Lambda_{\overline{\text{MS}}^2}^2} - \frac{a_1}{\beta_0} \right)$ and therefore

$$\Lambda_V(n_f) = \Lambda_{\overline{\text{MS}}}(n_f) \exp \left(-\frac{a_1}{2\beta_0} \right). \quad (15)$$

This relation gives

$$\begin{aligned}\Lambda_V(n_f = 3) &= 1.4753 \Lambda_{\overline{MS}}(n_f = 3), \\ \Lambda_V(n_f = 4) &= 1.4238 \Lambda_{\overline{MS}}(n_f = 4), \\ \Lambda_V(n_f = 5) &= 1.3656 \Lambda_{\overline{MS}}(n_f = 5).\end{aligned}\tag{16}$$

If one takes the perturbative $\Lambda_{\overline{MS}}(n_f)$ from Eq. (4), then the following values for the “vector” constants in pQCD are obtained:

$$\begin{aligned}\Lambda_V(n_f = 5) &= (291 \pm 11) \text{ MeV}, \\ \Lambda_V(n_f = 4) &= (421 \pm 15) \text{ MeV}, \\ \Lambda_V(n_f = 3) &= (500 \pm 15) \text{ MeV}.\end{aligned}\tag{17}$$

For our purpose it is more convenient to make the matching procedure for the coupling $\alpha_B(q^2)$ in momentum space, not for $\alpha_s(q^2)$. It is interesting to underline that in this case the calculated values of $\Lambda_V(n_f)$ for $n_f = 4, 5$ practically coincide with their values in Eq. (17), although now the IR regulator is taken into account.

We give below two sets of $\Lambda_V(n_f)$ for two different values of M_B , equal to 1.15 and 1.0, namely, if $M_B = 1.15 \text{ GeV}$

$$\Lambda_V(n_f = 5) = 310 \text{ MeV}, \quad \Lambda_V(n_f = 4) = 429.6 \text{ MeV}, \quad \Lambda_V(n_f = 3) = 497.4 \text{ MeV}, \tag{18}$$

and if $M_B = 1.00 \text{ GeV}$

$$\Lambda_V(n_f = 5) = 315 \text{ MeV}, \quad \Lambda_V(n_f = 4) = 435 \text{ MeV}, \quad \Lambda_V(n_f = 3) = 499.7 \text{ MeV}. \tag{19}$$

One can see that the fitted values of $\Lambda_V(n_f)$ weakly depend on the IR regulator M_B , taken in the range $(1.0 - 1.15) \text{ GeV}$, changing within $\pm 5 \text{ MeV}$. (Here the matching was performed at the quark mass thresholds: $q_{54} = 4.20 \text{ GeV}$ and $q_{43} = 1.50 \text{ GeV}$.) The difference between these two sets becomes manifest in the frozen value: $\alpha_{\text{crit}}(q = 0, n_f = 3) = 0.630$ for $M_B = 1.15 \text{ GeV}$ and $\alpha_{\text{crit}} = 0.819$ for $M_B = 1.0 \text{ GeV}$.

In Fig. 1 we show the coupling $\alpha_B(q^2)$ with $M_B = 1.15 \text{ GeV}$ and $\Lambda_V(n_f)$ from Eq. (18). For a comparison we shall also use the set with a smaller $\Lambda(n_f = 3) = 465 \text{ MeV}$,

$$\Lambda_V(n_f = 5) = 292 \text{ MeV}, \quad \Lambda_V(n_f = 4) = 406 \text{ MeV}, \quad \Lambda(n_f = 3) = 465 \text{ MeV}, \tag{20}$$

and a smaller $\alpha_{\text{crit}}(q^2 = 0, n_f = 3) = 0.5712$.

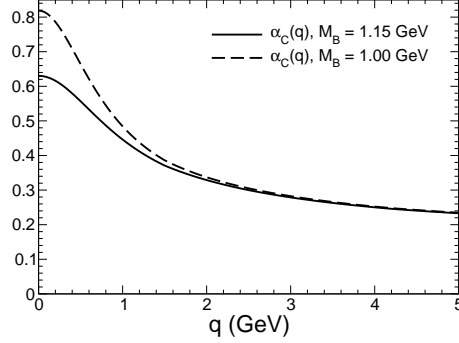


FIG. 1: Compound $\alpha_B(q)$ for $M_B = 1.15$ GeV and $\Lambda_V(n_f)$ from Eq. (18) and for $M_B = 1.00$ GeV and $\Lambda_V(n_f)$ from Eq. (19).

We give in Fig. 1 two curves for the compound $\alpha_B(q^2)$ with the parameters taken from Eqs. (18) and (19).

The freezing phenomenon of the vector coupling was widely used in phenomenology [2–5], where typical values $\alpha_{\text{crit}} \sim 0.54 - 0.60$ were used. However, in the lattice static potential much smaller values $\alpha_{\text{crit}} \equiv \alpha(\text{lat})$ were measured: $\alpha(\text{lat}) \sim 0.22$ in quenched QCD ($n_f = 0$) [28] and $\alpha(\text{lat}) \sim 0.30$ in full QCD [29]. The reason for that discrepancy possibly comes from lattice artifacts, present in the lattice GE potential, and also from an additional normalization condition, usually put on the lattice static potential [24, 30].

Also in some lattice potentials saturation of the vector coupling takes place at very small distances, $r \sim 0.2$ fm [18], [28], while in our approach the vector coupling is approaching its critical value at much larger $r \gtrsim 0.6$ fm (see Figs. 2,3). Our present result agrees with the lattice study of the function $c(r)$ in Ref. [31], which will be discussed in Sect. V.

From Eq. (17) it is evident that the asymptotic coupling α_{crit} is fully determined by the ratio $\eta^2 = \frac{M_B}{\Lambda_V^2}$ and in two-loop approximation is given by

$$\alpha_B(q=0) = \frac{4\pi}{\beta_0 t_0} \left(1 - \frac{\beta_1}{\beta_0^2} \frac{\ln t_0}{t_0} \right), \quad (21)$$

with the logarithm

$$t_0 = \ln \eta^2 = \ln \left(\frac{M_B^2}{\Lambda_V^2} \right). \quad (22)$$

The critical value has to be determined with great accuracy. However, small uncertainties in the values of $\Lambda_V(n_f = 3)$ and M_B do not allow to fix $\alpha_{\text{crit}}(n_f = 3)$. As we have already mentioned, such a difference may reach $\sim 30\%$.

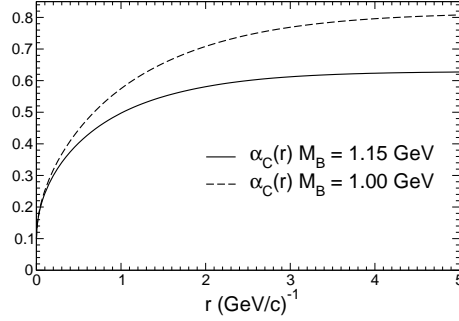


FIG. 2: Compound $\alpha_B(r)$ with $\alpha_{\text{crit}} = 0.63015$ and the parameters from Eq. (18) (solid line), and $\alpha_B(r)$ (dashed line) with $\alpha_{\text{crit}} = 0.819$ and the parameters from Eq. (19).

It is important that the critical couplings in the momentum and the coordinate spaces coincide:

$$\alpha_B(\text{crit}) = \alpha_B(r \rightarrow \infty) = \alpha_B(q = 0). \quad (23)$$

It is of interest to understand why in phenomenological models the smaller values $\Lambda_V(n_f = 3) \sim 330 - 380$ MeV are often used (compare to those from (17)), giving, nevertheless, a good description of the low-lying meson states. Such values of Λ_V correspond to a smaller $\Lambda_{\overline{\text{MS}}}(n_f = 3) \sim 250$ MeV, as compared to that from Eq. (4), and close to those, calculated in the quenched approximation on the lattice, $\Lambda(n_f = 0) = (245 \pm 20)$ MeV [25]. Nevertheless, in this case a reasonable agreement with experiment is reached due to the small value taken for M_B and the large value of the freezing constant, $\alpha_B(\text{crit}) \sim 0.60$.

IV. THE VECTOR COUPLING IN THE COORDINATE SPACE

The vector coupling in the coordinate space is defined according to Eq. (3), where the integral can be rewritten in a different way, introducing the variable $y = \frac{q}{\Lambda_V}$,

$$\alpha_B(r\Lambda_V, \eta^2) = \frac{2}{\pi} \int_0^\infty dy \frac{\sin(r\Lambda_V y)}{y} \alpha_B(y, \eta^2), \quad (24)$$

This expression explicitly shows that $\alpha_B(r)$ depends on the combination $r\Lambda_V(n_f)$, if n_f is fixed, and also on the parameter $\eta^2 = \frac{M_B^2}{\Lambda_V(n_f)^2}$.

In Fig. 2 two couplings $\alpha_B(r)$ are shown for two sets of $\Lambda(n_f)$ from Eqs. (18), (19), where the critical values are equal to 0.630 ($M_B = 1.15$ GeV) and 0.819 ($M_B = 1.0$ GeV).

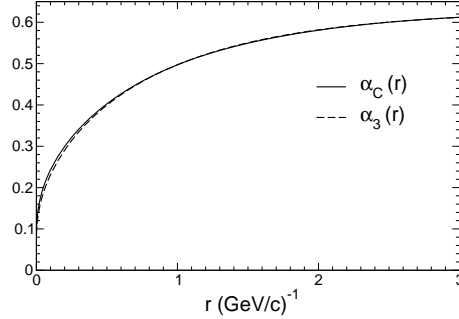


FIG. 3: Comparison of the compound $\alpha_B(r)$ with parameters from Eq. (18) and $\alpha_B(r)$ with fixed $n_f = 3$ and the same α_{crit} and $\Lambda_V(n_f = 3) = 0.4974$ GeV.

In Fig. 3 the calculated “compound” $\alpha_B(r)$ with $M_B = 1.15$ GeV is compared to the coupling $\alpha_B(r)$, in which $n_f = 3$ is fixed (no matching), while for both couplings their critical values coincide and are equal to 0.630. As seen from Fig. 3, both curves are very close to each other and, perhaps just owing to this fact, the vector coupling with fixed n_f may be used in phenomenological models. It also indicates that the frozen value of the coupling is of primary importance.

Notice that the situation is different for light and strange mesons, which have large sizes, and for them a screening of the GE interaction is possible, which can occur owing to open channels, decreasing the vector coupling.

V. THE STATIC FORCE AND THE FUNCTION $c(r)$

To have an additional test of the calculated vector coupling $\alpha_B(r)$ we consider here the static force,

$$F_B(r) = V'_{\text{st}}(r) = \sigma + V'_{GE}(r) \equiv \sigma + \frac{4}{3} \frac{\alpha_F(r)}{r^2}, \quad (25)$$

where the coupling

$$\alpha_F(r) = \alpha_B(r) - r\alpha'_B(r) \quad (26)$$

is introduced. The values of $\alpha_F(r)$ are smaller as compared to $\alpha_B(r)$ since the derivative $\alpha'_B(r)$ is positive.

In Fig. 4 the coupling $\alpha_F(r)$ together with $\alpha_B(r)$ with parameters from (18) are shown; one can see that $\alpha_F(r)$ is smaller by $\sim 20\%$ in the region $(0.5 - 0.6)$ fm.

To compare our results with the existing lattice data we introduce the dimensionless

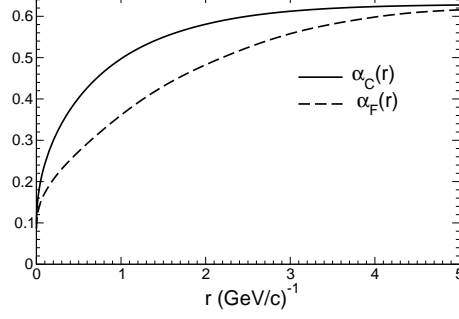


FIG. 4: The compound $\alpha_F(r)$ and $\alpha_B(r)$, taking $\Lambda_V(n_f)$ from Eq. (18) with $M_B = 1.15$ GeV, $\Lambda_V(n_f = 3) = 0.4974$ GeV, and $\alpha_{\text{Bcrit}} = 0.63015$.

function $r^2 F_B(r)$ and calculate two characteristic scales: r_1 and r_0 [32]:

$$r_1^2 F_B(r_1) = 1.0, \quad r_0^2 F_B(r_0) = 1.65, \quad (27)$$

where the function

$$r^2 F_B(r) = r^2 \sigma + \frac{4}{3} \alpha_F(r), \quad (28)$$

depends both on σ and $\alpha_F(r)$. For the static potential, like the Cornell and some lattice potentials, with the coupling constant equal to a constant, one has $\tilde{V}_{\text{st}}(r) = \sigma r - \frac{e}{r}$ (where $e = \frac{4}{3} \alpha(\text{lat}) = \text{constant}$) and therefore in the static force,

$$\tilde{F}(r) = \sigma + \frac{e}{r^2}, \quad (29)$$

the coupling $\alpha_F = \frac{3}{4}e$ is also constant.

On the contrary, in our calculations the coupling $\alpha_F(r)$ changes rapidly in the region $0 \leq r \leq 0.4$ fm, approaching $\alpha_B(r)$ only at large distances $r \geq 0.8$ fm (see Fig. 4, where $\Lambda_V(n_f)$ is taken from Eq. (18) with $M_B = 1.15$ GeV).

From Eq. (29) one easily calculates the characteristic sizes:

$$r_1 = 1.530 \text{ GeV}^{-1} = 0.303 \text{ fm}, \quad r_0 = 2.321 \text{ GeV}^{-1} = 0.460 \text{ fm}. \quad (30)$$

These scales r_1 , r_0 for $\Lambda_V(n_f = 3) = 497.4$ MeV, which correspond to the central value of the perturbative $\Lambda_{\overline{\text{MS}}}(n_f = 3) = 337$ MeV, appear to be very close to those calculated on the lattice: $r_1(\text{lat}) = 1.621 \text{ GeV}^{-1} = 0.321 \text{ fm}$ [33] and $r_0 = 1.3656(20) \text{ GeV}^{-1} = (0.468 \pm 0.004) \text{ fm}$ [24], being only several percents smaller. However, to reach precise agreement with the lattice scales one needs to take a bit smaller $\Lambda_{\overline{\text{MS}}}(n_f)$, namely, those

values which correspond to the lower bounds in pQCD (4): $\Lambda_{\overline{\text{MS}}}(n_f = 5, 2\text{-loop}) = 208 \text{ MeV}$, $\Lambda_{\overline{\text{MS}}}(n_f = 4) = 279.2 \text{ MeV}$, $\Lambda_{\overline{\text{MS}}}(n_f = 3) = 322 \text{ MeV}$. For this choice we have obtained $\alpha_{\text{crit}} = 0.5712$, $r_1 = 0.312 \text{ fm}$, and $r_0 = 0.470 \text{ fm}$, which coincide with the lattice scales from Refs. [33], [34] with an accuracy better than 3%.

In the cases considered we have found the following values for the product $r_0 \Lambda_{\overline{\text{MS}}}(n_f = 3)$:

$$\begin{aligned} r_0 \Lambda_{\overline{\text{MS}}}(n_f = 3) &= 0.764, \quad \text{for } r_0 = 0.470 \text{ fm}, \quad \alpha_{\text{crit}} = 0.5712, \\ r_0 \Lambda_{\overline{\text{MS}}}(n_f = 3) &= 0.782, \quad \text{for } r_0 = 0.460 \text{ fm}, \quad \alpha_{\text{crit}} = 0.630, \end{aligned} \quad (31)$$

in good agreement with the lattice results from Refs. [33, 34]. Thus we conclude that for large $\Lambda_V(n_f = 3) \sim 500 \text{ MeV}$, with the corresponding $\Lambda_{\overline{\text{MS}}} = 0.339 \text{ MeV}$, one needs to take a relatively large IR regulator $M_B = 1.15 \text{ GeV}$ to obtain the scales r_1 , r_0 in agreement with the lattice results.

For a smaller regulator, e.g. $M_B = 1.0 \text{ GeV}$, the scales r_1 , r_0 turn out to be smaller: $r_1 = 0.292 \text{ fm}$ and $r_0 = 0.442 \text{ fm}$ and the product $r_0 \Lambda_{\overline{\text{MS}}}(n_f = 3) = 0.757$.

On the contrary, the large value $r_0 = 0.50 \text{ fm}$ may be obtained in two ways: either with larger regulator $M_B \gtrsim 1.30 \text{ GeV}$, if the ‘‘perturbative’’ $\Lambda_{\overline{\text{MS}}}(n_f = 3)$ from Eq. (4) are used, or taking the significantly smaller value of $\Lambda_{\overline{\text{MS}}}(n_f = 3) \sim 245 \text{ MeV}$, as in the quenched lattice calculation [25].

Thus we can conclude that the scale r_0 cannot be considered as a universal parameter but depends on Λ and M_B used. Notice, that the force $F_B(r)$ depends also on the string tension and our calculations were performed with $\sigma = 0.18 \text{ GeV}^2$, having obtained for the scales r_1 and r_0 a good agreement with the lattice results.

An additional and very important test of the vector coupling comes from the study of the function $c(r)$, defined via the second derivative of the static potential and therefore it does not depend on the string tension. It is determined by $\alpha_B(r)$ and its first and second derivatives:

$$c(r) = \frac{1}{2} r^3 V_{\text{st}}''(r) = -\frac{4}{3} \alpha_F(r) - \frac{4}{3} \alpha_B''(r) \frac{r^2}{2}. \quad (32)$$

The second derivative $\alpha_B''(r)$ is negative and therefore the magnitude of $c(r)$ appears to be smaller than that of $\frac{4}{3} \alpha_F(r)$. Moreover, the slope of $c(r)$ depends on the IR regulator used. The behavior of $c(r)$ is shown in Fig. 5 together with the points taken from the lattice calculations with $n_f = 2$ from Ref. [35]. One can see the good agreement with both results.

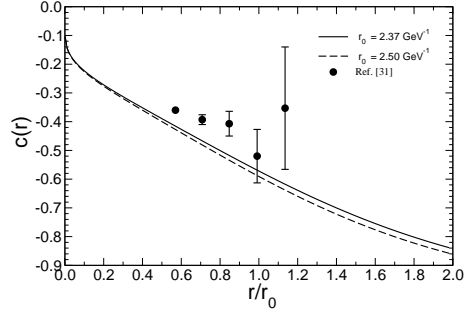


FIG. 5: The function $c(r)$ for $M_B = 1.15$ GeV and $\Lambda_V(n_f)$ from Eq. (18); the points with the errors are taken from Ref. [31], where the function $c(r)$ was calculated on the lattice with $n_f = 2$.

VI. THE BOTTOMONIUM SPECTRUM AS A TEST OF α_{crit}

In bottomonium the centroid mass $\bar{M}(nl)$ for a given multiplet nl just coincides with the e.v. $\bar{M}(nl)$ of the Hamiltonian (8):

$$\left[2\sqrt{\mathbf{p}^2 + m_b^2} + V_{\text{st}}(r) \right] \varphi_{nl} = \bar{M}(nl) \varphi_{nl}. \quad (33)$$

Here we perform calculations with the use of the SSE, since in the relativistic case the accuracy is better than in the nonrelativistic and so-called einbein approximations, although the difference between them is only several MeV for low-lying masses $\bar{M}(nl)$ and their mass splittings.

The bottomonium spectrum was calculated taking the compound $\alpha_B(r)$ with the values of $\Lambda_V(n_f)$ from (18) and also in the case with fixed $n_f = 3$ and the same $\Lambda_V(n_f = 3) = 497.4$ MeV, but without matching. It appears that the differences between the masses calculated in these two cases are very small, $\sim 2 - 6$ MeV. Therefore it is of special importance to consider a different $\Lambda_V(n_f = 3)$, or a different $\Lambda_{\overline{\text{MS}}}(n_f = 3)$. Our calculations show that there are several mass splittings, which are most sensitive to the choice of the ratio $\eta^2 = \frac{M_B^2}{\Lambda_V^2}$, determining the frozen value of $\alpha_B(r)$. Their experimental values are taken from [15, 36, 37]:

$$\begin{aligned} \bar{M}(2P) - \bar{M}(1P) &= (360.0 \pm 1.7) \text{ MeV}, \\ \bar{M}(3P) - \bar{M}(2P) &= (280 \pm 14) \text{ MeV}, \\ \bar{M}(1D) - \bar{M}(1P) &= \Delta = (264 \pm 2) \text{ MeV}. \end{aligned} \quad (34)$$

Here the centroid mass $\bar{M}(\chi_b(3P)) \simeq (10540 \pm 5)$ MeV is estimated from two experimental masses measured by the ATLAS [36] and the D0 [37] collaborations.

In Ref. [38] it was already demonstrated that the fit to the bottomonium splittings appears to be sensitive to choice of the critical coupling constant. However, in the vector couplings the parameters were often taken in a rather arbitrary way. In particular, for the lattice static potential with small $\alpha_{\text{lat}}(r) = \text{const} = 0.306$ ($n_f = 3$) [29] the $1D - 1P$, $1P - 1S$ splittings are $40 \div 30$ MeV smaller than their experimental values.

First we determine the masses of the $1D$ multiplet. The fine-structure splittings of this multiplet were calculated taking the strong coupling in the spin-orbit and tensor interaction as for the $1P$ -states [27], namely, $\alpha_s(\mu_{\text{FS}}) = 0.38 \pm 0.02$ at the scale $\mu_{\text{FS}} \sim 1$ GeV. The following masses were obtained,

$$\begin{aligned} M(1^3D_3) &= (10270 \pm 2) \text{ MeV}, \\ M(1^3D_2) &= (10264 \pm 2) \text{ MeV}, \\ M(1^3D_1) &= (10254 \pm 3) \text{ MeV}, \end{aligned} \tag{35}$$

so that the calculated centroid mass is by ~ 1 MeV larger than $M(1^3D_2) = (10163 \pm 2)$ MeV, known from experiments, $\bar{M}(1D) = (10164 \pm 2)$ MeV. Here we would like to notice that in our calculations the splittings of the $1D$ multiplet (35) are two times smaller than those in lattice calculations [39].

For the nP bottomonium multiplets their spin-averaged masses are known very accurately [15, 40, 41]:

$$\bar{M}(1P) = (9900.0 \pm 0.6) \text{ MeV}, \quad \bar{M}(2P) = (10260 \pm 0.7) \text{ MeV}, \tag{36}$$

and therefore the mass splitting $\bar{M}(2P) - \bar{M}(1P) = 260(2)$ MeV is also known with great accuracy.

As seen from Table I, the $1D - 1P$ splitting is in good agreement with experiment, close to the experimental value for $M_B = 1.10$ GeV, however, at the same time the $2P - 1P$ splitting increases and one needs to reach the best agreement for both splittings. Choosing different sets of the parameters M_B and $\Lambda_V(n = 3)$, we have observed that a good agreement with experimental splittings takes place in the cases with the freezing constant $\alpha_{\text{crit}} = 0.57 \pm 0.02$ and the IR regulator $M_B = (1.15 \pm 0.02)$ GeV, while the calculated spin-averaged masses coincide with experiment within $\pm(5 - 10)$ MeV accuracy. Notice, that the lattice

TABLE I: The mass splittings in bottomonium in MeV ($\Lambda_{\overline{\text{MS}}}(n=3) = 325$ MeV)

| | $M_B = 1.15$ GeV | $M_B = 1.10$ GeV | exp. [15] |
|-----------|-------------------|-------------------|--------------|
| State | $m_b = 4.832$ GeV | $m_b = 4.840$ GeV | |
| $1D - 1P$ | 259 | 261 | 264 ± 2 |
| $2P - 1P$ | 371 | 376 | 360 ± 2 |
| $3P - 2P$ | 288 | 294 | 280 ± 14 |

calculations give larger D -wave masses [39], as compared to ours, while smaller masses $M(1D)$ were predicted in Ref. [42].

For the $2P - 1P$ splitting a small deviation ~ 5 MeV from the experimental number can be obtained, if a smaller QCD constant $\Lambda_{\overline{\text{MS}}}(n=3) = (317 \pm 5)$ MeV is used, while $M_B = (1.15 \pm 0.02)$ GeV is relatively large.

We do not give here the centroid masses of the S -states, because for calculations of $\bar{M}(1S)$, $\bar{M}(2S)$ one needs to take into account the nonlinear behavior of confining potential at short distances, $r \lesssim 0.20$ fm and this fact gives rise to small negative corrections to the S -wave masses. Such corrections are very small for the states with $l \neq 0$, since their w.f.s are equal to zero near the origin, while the S -wave w.f.s have their maximum values there.

VII. CONCLUSIONS

We have studied the vector coupling in the momentum and coordinate spaces, introducing the IR regulator, $M_B = \sqrt{2\pi\sigma} = (1.06 \pm 0.11)$ GeV, as it is prescribed in BPTh.

For the vector coupling in momentum space we have performed the matching procedure at the quark mass thresholds and calculated the “vector” constants $\Lambda_V(n_f)$. It appears that these constants correspond to $\Lambda_{\overline{\text{MS}}}(n_f)$, which coincide with the perturbative $\Lambda_{\overline{\text{MS}}}(n_f)$ within ± 5 MeV; moreover, their values weakly depend on the regulator M_B , if it is taken from the range $(1.0 - 1.20)$ GeV.

The calculated scales r_0 and r_1 are shown not to be universal numbers and r_0 decreases by 6% when M_B decreases from the value $M_B = 1.15$ GeV to $M_B = 1.00$ GeV. The ratio $\frac{r_0}{r_1} = 1.505 \pm 0.02$ and the product $r_0 \Lambda_{\overline{\text{MS}}}(n_f=3) = 0.77 \pm 0.02$ are obtained.

The choice with $M_B = 1.15$ GeV and $\Lambda_{\overline{\text{MS}}}(n_f=3) = 322$ MeV gives the best (precise) agreement with the lattice scales r_0 and r_1

The function $c(r)$, which is proportional to the second derivative of the static potential and does not depend on the string tension, is calculated, and appears to be in agreement with the ALPHA Collab. predictions.

Our analysis of the bottomonium spectrum shows that the splittings $\bar{M}(1D) - \bar{M}(1P)$ and $\bar{M}(2P) - \bar{M}(1P)$ are very sensitive to the ratio $\eta^2 = \frac{M_B^2}{\Lambda_V(n_f=3)^2}$ used and the best agreement with experiment is reached taking $\eta = 2.46 \pm 0.04$, or $\alpha_{\text{crit}} = 0.57 \pm 0.02$.

The following splittings for the members of the bottomonium $1D$ multiplet are predicted: $M(1^3D_3) - M(1^3D_2) = 7(2)$ MeV, $M(1^3D_2) - M(1^3D_1) = 9(3)$ MeV.

Acknowledgments

The authors are grateful to Yu. A. Simonov for useful discussions and suggestions.

-
- [1] E. Eichten et al., Phys. Rev. D **21**, 203 (1980); Phys. Rev. Lett. **34**, 369 (1975).
 - [2] D. P. Stanley and D. Robson, Phys. Rev. D **21**, 3180 (1980); Phys. Rev. Lett. **45**, 235 (1980); L. P. Fulcher, Phys. Rev. D **44**, 2079 (1991); ibid D **50**, 447 (1994); J. L. Basdevant and S. Boukraa, Z. Phys. C **28** (1983).
 - [3] S. Godfrey and N. Isgur, Phys. Rev. D **32**, 189 (1985).
 - [4] D. Ebert, R. N. Faustov, and V. O. Galkin, Phys. Rev. D **67**, 014027 (2003); Mod. Phys. Lett. A **20**, 1887 (2005) .
 - [5] W. Lucha, F. F. Schoberl, and D. Gromes, Phys. Rept. **200**, 127 (1991) and references therein.
 - [6] A. Yu. Dubin, A. B. Kaidalov, and Yu. A. Simonov, Phys. Lett. B **323**, 41 (1994); Yad. Fiz. **56**, 213 (1993); E. Gubankova and A. Yu. Dubin, Phys. Lett. B **334**, 180 (1994) .
 - [7] Yu. A. Simonov, Nucl. Phys. B **307**, 512 (1988); G. Dosch and Yu. A. Simonov, Phys. Lett. B **205**, 339 (1988); Z. Phys. C **45**, 147 (1989).
 - [8] A. DiGiacomo, H. G. Dosch, V. I. Shevchenko, and Yu. A. Simonov, Phys. Rept. **372**, 319 (2002).
 - [9] A. M. Badalian and B. L. G. Bakker, Phys. Rev. D **66**, 034025 (2002).
 - [10] Yu. A. Simonov, Phys. Atom. Nucl. **74**, 1223 (2011); arXiv:1011.5386 (2010)[hep-ph].

- [11] A. M. Badalian and V. P. Yurov, Phys. Atom. Nucl. **56**, 176 (1993); Sov. J. Nucl. Phys. **51**, 869 (1990)
- [12] V. Shevchenko and Yu. A. Simonov, Phys. Rev. Lett. **85**, 1811 (2001); hep-ph/0104135 (2001).
- [13] G. S. Bali, Phys. Rev. D **62**, 114503 (2000).
- [14] M. Peter, Phys. Rev. Lett. **78**, 602 (1997); Nucl. Phys. B **501**, 471 (1997); Y. Schröder Phys. Lett. B **447**, 321 (1999).
- [15] J. Beringer et al. (Particle Data Group), Phys. Rev. D **86**, 010001 (2012).
- [16] S. Bethke, arXiv:1210.0325 (2012) [hep-ex] and references therein.
- [17] A. M. Badalian and D. S. Kuzmenko, Phys. Rev. D **65**, 2173 (2002); A. M. Badalian, Phys. Atom. Nucl. **63**, 2173 (2000). (2002)
- [18] G. Bali, Phys. Lett. B **460**, 170 (1999).
- [19] E. J. Eichten and C. Quigg, Phys. Rev. d **52**, 1726 (1995).
- [20] A. M. Badalian, I. V. Danilkin, and B. L. G. Bakker, Phys. Rev. D **79**, 037505 (2009); Phys. Atom. Nucl. **73**, 138 (2010).
- [21] G. Parisi and R. Petronzio, Phys. Lett. B **94**, 51 (1980); J. M. Cornwall, Phys. Rev. D **26**, 1453 (1982); A. C. Mattingly and P. M. Stevenson, Phys. Rev. D **49**, 437 (1994)..
- [22] D. V. Shirkov, arXiv:1208.2103 (2012) [hep-ph].
- [23] A. M. Badalian, B. L. G. Bakker, and I. V. Danilkin, Phys. Rev. D **81**, 071502 (2010);Erratum-ibid: D **81**, 099902 (2010); Phys. Atom. Nucl. **74**, 631 (2011).
- [24] V. Bazavov et al., arXiv:1205.6155 [hep-lat]; Phys. Rev. D **85**, 054503 (2012) and references therein.
- [25] S. Capitani, M. Luescher, R. Sommer, and H. Wittig, Nucl. Phys. B **544**, 669 (1999).
- [26] Yu. A. Simonov, Phys. Lett. B **515**, 137 (2001).
- [27] A. M. Badalian and B. L. G. Bakker, Phys. Rev. D **62**, 094031 (2000).
- [28] Y. Koma and M. Koma, Nucl. phys. B **769**, 79 (2007); G. Bali and K. Schilling, Phys. Rev. D **47**, 661 (1993); K. D. Born, E. Laerman, and T. F. Walsh, and P. M. Zerwas, Phys. Lett. B **329**, 325 (1994).
- [29] C. W. Bernard et al. (MILK Collab.), Phys. Rev. D **64**, 054506 (2001); ibid. Phys. Rev. D **62**, 034503 (2000).
- [30] C. T. H. Davies et al., Phys. Rev. D **81**, 034506 (2010); M. Cheng et al., Phys. Rev. D **81**, 054504 (2010).

- [31] M. Donnellan et al., Nucl. Phys. B **849**, 45 (2011) and references therein.
- [32] R. Sommer, Nucl. Phys. B **411**, 839 (1994).
- [33] A. Gray et al., Phys. Rev. D **72**, 094507 (2005).
- [34] R. J. Dowdall et al. (HPQCD Collab.), arXiv:1110.6887 (2011) [hep-lat].
- [35] P. Fritzsche, et al. (ALPHA Collab.), Nucl. Phys. B **865**, 397 (2012)
- [36] G. Aad et al. (ATLAS Collab.), Phys. Rev. Lett. **108**, 152001 (2012).
- [37] V. M. Abazov et al. (D0 Collab), Phys. Rev. D **86**, 031103 (2012).
- [38] A. M. Badalian, A. I. Veselov, and B. L. G. Bakker, Phys. Rev. D **70**, 016007 (2004).
- [39] J. O. Daldrop, C. T. H. Davies, and R. J. Dowdall, arXiv:1112.2590 (2011) [hep-lat].
- [40] G. Bonvicini et al. (CLEO Collab.), Phys. Rev. D **70**, 032001 (2004).
- [41] P. Del Amo Sanchez et al. (BaBar Collab.), Phys. Rev. D **82**, 111102 (R) (2010).
- [42] W. Kwong and J. L. Rosner, Phys. Rev. D **38**, 279 (1988).